PHYSICAL REVIEW D VOLUME 43, NUMBER 7 1 APRIL 1991

Kinematically covariant calculation of meson form factors

A. Ilakovac and D. Tadić
Department of Theoretical Physics, Prirodoslovno-matematički fakultet, Marulićev trg 19, Zagreb, Croatia, Yugoslavia
(Received 27 September 1990)

Hadron form factors are calculated in the relativized version of the MIT bag model. The model, without any additional fitting parameters, gives acceptable values for proton and pion electromagnetic form factors. Theoretical predictions for K-, D-, and B-meson form factors are compared with other theoretical results and with the experimental data for semileptonic decays.

I. INTRODUCTION

The exclusive semileptonic decays not only provide an excellent way to determine the Kobyashi-Maskawa matrix elements V_{ij}, but also open a view on the intricacies of QCD. As the underlying quark dynamics is probed by weak currents, semileptonic decays give direct information on the internal structure of mesons.

This paper is based on the quark model approach. It uses a simple, but nevertheless relativistically covariant, model.[1-3] A detailed description of such a model has already been published.[2-4] For the convenience of the reader, the model's main features are described in the next section where it is also tested by calculating some experimentally well-known hadron form factors.

Our reliance on the constituent quark model, which is a phenomenological model of QCD in the nonperturbative regime, is partially based on the successes which this model has had in describing hadron structure. Quark models have also been used before[5-14] as a basis for momentum-dependent calculations. Some additional discussion can be found in Refs. 2 and 3.

Additional motivation can be found in Refs. 15 and 16 where the perturbative QCD contributions and free-quark decay model are discussed. Reference 15 argued that perturbative contributions are much smaller than soft nonperturbative ones. The nonperturbative contributions were approximately estimated by using the quark model. They[15] even concluded that there is no justification for the continued application of perturbative QCD to exclusive processes. Reference 16 stressed that QCD-perturbed free-quark calculations contain extra parameters introduced to describe bound-state effects, which actually control the theoretical predictions. The fact that the experimental spectrum for the decay $\bar{B} \to Xe\bar{\nu}$ seems to be dominated by D and D^* production[16] speaks in favor of a model which describes mesons as bound $q\bar{q}$ states.

QCD sum-rule methods,[17] which avoid the main flaws of the quark models, indicate that both the nucleon and pion electromagnetic form factors are dominated, at measured Q^2, by nonperturbative contributions. Similar methods[18] produce $B \to D^*$ transition form factors which are in reasonable agreement with our results (see Sec. IV).

Numerous imperfections in the quark-model-based calculations reflect the state of our present understanding of nonperturbative QCD. Obviously, any quark model could be improved by including higher Fock-state contributions, which might be quite important for a better description of the pion.

As will be shown, our model can reasonably well reproduce the pion form factor. The simple choice of only one Fock state seems to be compensated by the mock-meson[16] character of the model wave functions. The same effect seems to lead to the results obtained by Ref. 16. It is encouraging that diverse models lead to very similar results.

The plethora of the suggested quark models, for which some examples can be found in Refs. 16 and 18–31, indicates that presently one can make only some guesses about nonperturbative QCD. This theoretical uncertainty provides a motivation to explore some additional models, such as the one presented in this paper. But there are other more pragmatic reasons.

When calculating form factors, one has to solve various dynamical and kinematical problems. Thus it might be useful to develop a model which is covariant, although its dynamics is quite rudimentary.

Our model is based on the standard MIT bag model. It uses only MIT bag model parameters. In the zero-meson-momentum limit ($\mathbf{P}=0$), it is identical to the bag model. Several variants of the model were developed and tested in the $\mathbf{P}\neq 0$ region.

Comparisons were made with other models. An acceptable agreement was found with models[16,19-31] whose common features are valence-quark states and simple, quasifree, particle dynamics. One ventures to say that the theoretical predictions for the low-momentum transfer, based on the valence-quark models in the weak-binding limit,[16] are to a large extent independent of the detailed structure of a given model.

II. MODEL DESCRIPTION AND TESTING

In principle, the so-called "bola"[1] version of the bag model[2,3] (BBM) is connected with the quasipotential approximation[2,32] of the Bethe-Salpeter equation. In our paper this model is used as a very simple generalization of the static MIT bag (MB) model.[33] The same approach[1]

can be used to relativize any potential model. Precisely speaking, one refers to the models in which particles (i.e., quarks) are confined inside some potential (or enclosure in the case of MB model). Otherwise, they are independent of each other. The role of a central potential (or a bag) is played by an additional scalar spurion. This spurion does not contribute to any physical process. Its presence results in a condition on the coordinate and momentum of the center of the potential (or bag), thus ensuring overall energy-momentum conservation. In the quantum field version of the model,[33] the quark creation (annihilation) operators must refer to the particular, initial or final, bag. The contraction of the two operators, which are not "caught" by the weak current, and which belong to two different bags, produces an overlap factor [see Eq. (2.6) below]. They are caught by an overlap operator $\int \bar{\psi}\gamma\psi\delta(Lz)d^4z$. (Here ψ's are quark-field operators and the rest are explained below.) The overlap factors Z appear naturally when one uses a meson wave function [see (2.1) below].

A detailed description of the calculation of the hadron form factors in the BBM has already been published.[3,4] Only some essential steps will be outlined here.

The two-quark wave function, describing a meson, has a generic form:

$$\psi_P(y,z_1,z_2)=N_P\exp(-iPy)\psi_1(z_1^P)\bar{\psi}_2(z_2^P)\ ,$$
$$\psi(z^P)=S(P)\eta(z_\perp^P)\exp(-iz_\parallel^P\epsilon)\ . \tag{2.1}$$

Here ϵ is the static bag (or potential model) energy and N_P is a norm. $S(P)$ is the boost matrix

$$S(P)=(\not{P}\gamma^0+M)/[2M(E+M)]^{1/2}\ . \tag{2.2a}$$

The z^P are internal coordinates defined by[1,34]

$$x=y+z\ ,$$
$$z_\perp^\mu(P)=z^\mu-\beta^\mu(\beta\cdot z),\quad \beta_\mu=P_\mu/M\ , \tag{2.2b}$$
$$z_\parallel(P)=\beta_\mu z^\mu\ .$$

The masses appearing in (2.2) can be either physical meson masses

$$M=m_x,\quad x=\pi,K,D,B \tag{2.3}$$

or the mock-meson[16] masses

$$M=\tilde{M},\quad \tilde{M}=\epsilon_r+\epsilon_s\ . \tag{2.4}$$

Here ϵ_i's correspond to the valence quarks.

With either choice the model leads to covariant results. The choice (2.4) might be the more consistent one as $\tilde{M}$ is the mass which emerges when the Bogoliubov model is solved.[33] With (2.4) one has a complete analogy with the mock-meson model of Ref. 16. One can also find some theoretical arguments in favor of the version (2.3). In the MIT bag model, the physical meson masses are reproduced[33] by adding to the ϵ's some perturbative terms, which do not influence the shape of the quark wave functions. From our point of view, the final choice must depend on the comparison with experimental data.

In the rest frame the quark function is of the form

$$\eta(\mathbf{r})=\begin{bmatrix} iU(|\mathbf{r}|)\chi \\ (\boldsymbol{\sigma}\cdot\mathbf{r}/|\mathbf{r}|)V(|\mathbf{r}|)\chi \end{bmatrix}\ . \tag{2.5}$$

Here χ is the Pauli spinor.

The covariant expression for an electroweak vertex has a generic form

$$V_\mu(P_f,P_i)=F_{\rm fl}\int d^4z_1d^4z_2d^4y\prod_{i=1}^{2}\delta(L\cdot z_i)\bar{\psi}_{P_f}(y,z_1,z_2)$$
$$\times\sum_{\text{perm } i,j=1}^{2}(O_\mu)_i e^{-iQx_1}(\gamma\cdot L)_j\psi_{P_i}(y,z_1,z_2)$$
$$=(2\pi)^4\delta^4(P_f-P_i-Q)N_{fi}I_{O_\mu}^{b_f a_i}Z^a\ , \tag{2.6a}$$
$$O_\mu=\gamma_\mu\ \text{ or }\ \gamma_\mu\gamma_5\ ,$$

and

$$I_{O_\mu}^{b_f a_i}=\int d^4z\,\delta(L\cdot z)\bar{\eta}_f(\mathbf{r}_f)S^{-1}(P_f)O_\mu S(P_i)\eta_i(\mathbf{r}_i)$$
$$\times\exp[i\arg(I)]\ ,$$
$$\arg(I)=\epsilon_f^{b_f}z_f^\parallel-\epsilon_i^{a_i}z_i^\parallel-Q\cdot z\ , \tag{2.6b}$$
$$N_{fi}=[M_fM_i/(2\pi)^3E_fE_i]^{1/2}\ .$$

The overlap factor Z^a is obtained from I_{O_μ} by the substitution

$$O_\mu\to L\cdot\gamma\ ,$$
$$\arg(I)\to\arg(Z^a)=\epsilon_f^a z_f^\parallel-\epsilon_i^a z_i^\parallel\ . \tag{2.6c}$$

The factor $F_{\rm fl}$ is connected with the spin-flavor structure of mesons and weak currents.

The four-vector L selects a particular interaction hypersurface which is introduced in the quasipotential approximation to the Bethe-Salpeter equation.[2,3,32,34] We have shown in Ref. 3 that the hypersurface defined by

$$L\cdot z=0\ ,$$
$$L^\mu=(\beta_i^\mu+\beta_f^\mu)/[(\beta_i+\beta_f)^2]^{1/2} \tag{2.7}$$

satisfies the conserved vector current (CVC) constraint.

An obvious three-quark generalization of the formula (2.6), which can be found in Ref. 3, gives a reasonable reproduction of the proton electromagnetic form factors. They are defined by

$$\langle B_f|V^\mu|B_i\rangle=\bar{U}_f[f_1(Q^2)\gamma^\mu+f_2(Q^2)i\sigma^{\mu\nu}Q_\nu$$
$$+f_3(Q^2)Q^\mu]U_i\ . \tag{2.8a}$$

The condition (2.7) gives

$$f_3(Q^2)\equiv 0\ , \tag{2.8b}$$

for any Q, as required by CVC.

The form factors were calculated using either physical

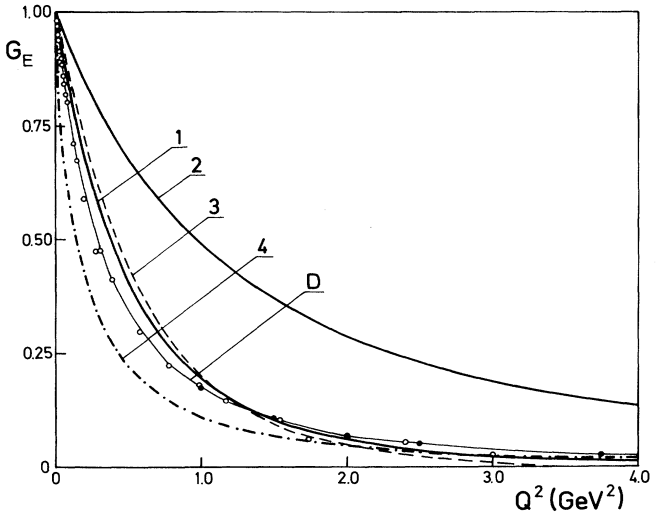

FIG. 1. Form factor G_E, calculated for various theoretical cases (explained in the text), is compared with the dipole formula. Experimental points are from Ref. 35.

proton mass M_P or the mock-proton mass

$$\tilde{M}_p = 2\epsilon_u + \epsilon_d \ .$$

The usage of the mock mass means some reparametrization of the Q^2 dependence of the form factors. In Fig. 1 Sach's form factor

$$G_E = f_1(Q^2, M_x) + \frac{Q^2}{2M_p} f_2(Q^2, M_x) \ ,$$

$$M_x = M_p \ \text{ or } \ \tilde{M}_p \ ,$$

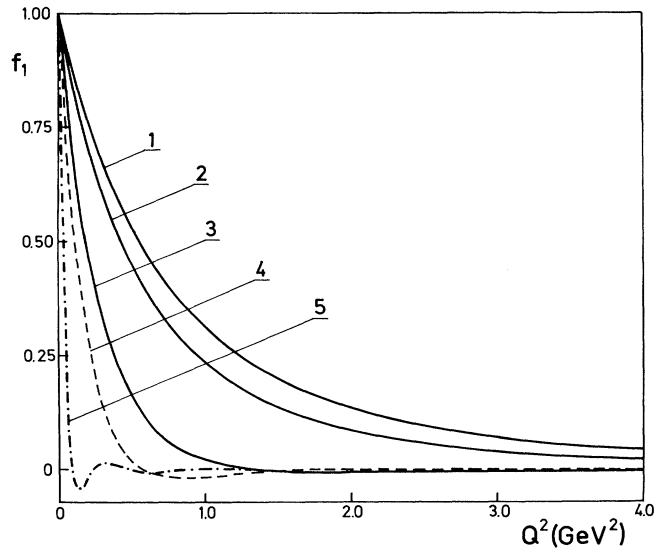

FIG. 2. Form factor $f_1(Q^2)$ is calculated for bag radii: (1) 2 GeV^{-1}, (2) 5 GeV^{-1}, (3) 8 GeV^{-1}, (4) 10 GeV^{-1}, and (5) 20 GeV^{-1}.

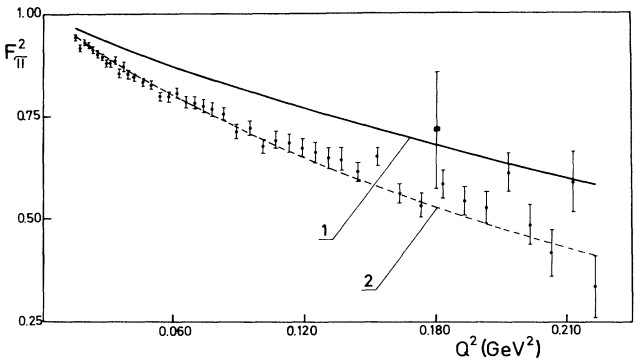

FIG. 3. Pion electromagnetic form factor squared $F^2_+(Q^2)$ is compared with experimental points of Refs. 37 and 38. Curve (1) corresponds to $\tilde{M}_\pi$, $Z=1$, and curve (2) to $\tilde{M}_\pi$, $Z\neq 1$.

is compared with the dipole formula.[35] Four curves are displayed:

(1) M_p, $Z\neq 1$,

(2) M_p, $Z=1$,

(3) $\tilde{M}_p$, $Z\neq 1$,

(4) $L^\mu=(1,0,0,1)$, M_p, $Z\neq 1$.

Curve (1) is in the best agreement with the dipole fit $D(Q^2)$. Up to $Q^2=1.40$ GeV^2 ($Q=1.18$ GeV), the discrepancy is always less than 20%. In the same region the mock-mass curve (3) is off for less than 25%. Curve (2), without the overlap factor correction, shows disastrous disagreement with $D(Q^2)$. At $Q^2=0.80$ GeV^2, for example, the mismatch is 150%. [The corresponding numbers for curves (1) and (3) are 15.8% and 22.2%, respectively.]

Curve (4) was loosely inspired by the null-plane ap-

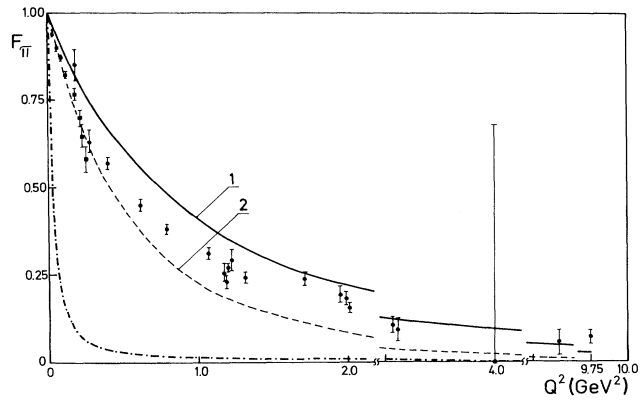

FIG. 4. Pion electromagnetic form factor $F_+(Q^2)$ is compared with experimental points of Refs. 37 and 38. Theoretical curves are (1) $\tilde{M}_\pi$, $Z=1$; (2) $\tilde{M}_\pi$, $Z\neq 1$. The dot-dashed curve is for M_π, $Z=1$.

TABLE I. $K \to \pi$ form factors.

Case	Z	Masses	λ_+	λ_0	$\zeta(0)$
1	$\neq 1$	Phys.	0.159	0.112	−0.551
2	$=1$	Phys.	0.079	0.033	−0.551
3	$\neq 1$	Mock	0.027	0.015	−0.156
4	$=1$	Mock	0.016	0.004	−0.156

proaches.[15,19,20] Our results correspond to

$$L^\mu=(1,0,0,1)\ , \tag{2.9}$$

in the Breit frame of reference. It is not exactly equivalent to the null-plane approaches. With the choice (2.9), the Z factor falls off very fast with Q^2. The calculated G_E is between 80% and 130% smaller than the one calculated by formula (2.7). The null-plane calculation does not agree with the CVC constraint (2.8b), as one obtains $f_3(Q^2)\neq 0$.

All curves were calculated using the proton-bag radius $R=5$ GeV^{-1}. This radius is also favored by the static proton data. In Fig. 2 we show the form factor $f_1(Q^2)$ calculated for various R's with $M=M_p$ and $Z\neq 1$. The pathological behavior at large R's is a particular feature of the bag model. The oscillations, which are very apparent for completely unrealistic $R=20$ GeV^{-1}, are connected with the zeros[36] of the Bessel functions $U(r)$ and $V(r)$ (2.5).

Our model calculates reasonable values for the pion electromagnetic form factor $F_+^\pi(Q^2)$ only if the mock mass

$$\tilde{M}_\pi=\epsilon_u+\epsilon_d$$

is used. The expression for the pion electromagnetic vertex is

$$\langle \pi(p_2)|V_\mu|\pi(p_1)\rangle = F_+^\pi(Q^2)(p_1+p_2)_\mu + F_-^\pi(Q^2)(p_1-p_2)_\mu\ . \tag{2.10a}$$

With the hypersurface (2.7) our formalism gives

$$F_-^\pi(Q^2)\equiv 0\ , \tag{2.10b}$$

for any Q^2 as required by CVC.

The form factor F_+^π was calculated for all points which can be found in Refs. 37 and 38. In Figs. 3 and 4 this form factor is calculated for

(1) $\tilde{M}_\pi$, $Z=1$,

(2) $\tilde{M}_\pi$, $Z\neq 1$,

(3) M_π, $Z=1$.

In both mock-mass cases, the disagreement between the experiment and theory is less than 50% up to $Q^2=1.0$ GeV^2. Curve (2) shows the best agreement for small $|Q^2|$, as is shown in Fig. 3. The theoretical F_+^π [case (2)] agrees with almost all experimental points of Ref. 38 within the experimental errors.

The theoretical results for $K \to \pi$ form factors [see (3.1) and Appendix] agree best with the experimental data if one uses mock masses. It is customary to express the experimental results in terms of the coefficients $\lambda_\pm$, λ_0, and

TABLE II. Meson form factors.

Process	Q^2	Z	F_+	OHI[a]
$D \to K$	1.88	1	0.592	1.15
	0	1	0.319	1.23
	0	0.479	0.152	2.58
$D \to \pi$	3.01	1	1.59	1.69
	0	1	0.179	3.85
	0	0.135	0.0238	28.8
$B \to \bar{D}^0$	11.6	1	0.182	0.852
	0	1	0.122	0.904
	0	0.618	0.0752	1.46
$B \to \pi$	26.4	1	1.52	1.92
	0	1	0.0462	4.23
	0	0.058	0.0027	72.7

[a]The form factors of Ref. 20 divided by our corresponding values ($Q^2=Q^2_{\max},0$).

TABLE III. Meson form factors.

Process	Q^2	Z	g	f	a_+	OHV[a]	OHA_1[a]	OHA_2[a]
$D^+ \to K^{*0}$	0.955	1	0.151	0.861	−0.135	1.51	1.27	1.40
	0	1	0.121	0.810	−0.181	1.47	1.16	1.48
	0	0.774	0.0939	0.627	−0.0843	1.89	1.50	1.91
$D^+ \to \rho^0$	1.21	1	0.167	0.770	−0.145	1.66	1.39	1.27
	0	1	0.122	0.709	−0.106	1.60	1.21	1.38
	0	0.697	0.0847	0.494	−0.0735	2.30	1.74	1.98
$B^0 \to D^{*+}$	10.7	1	0.0246	0.982	−0.0236	0.828	0.962	0.805
	0	1	0.0170	0.862	−0.0164	0.878	0.844	0.887
	0	0.657	0.0112	0.566	−0.0108	1.34	1.29	1.35
$B^+ \to \rho^0$	20.3	1	0.0640	0.774	−0.0553	0.747	1.25	0.551
	0	1	0.0142	0.458	−0.0128	0.956	0.947	0.900
	0	0.263	0.0037	0.121	−0.0034	3.63	3.48	3.42

[a]The form factors of Ref. 20 derived by our corresponding values ($Q^2=Q^2_{\max},0$).

$\zeta(0)$, which are defined by[39]

$$F_\pm(Q^2)=F_\pm(0)\left[1+\lambda_\pm\frac{Q^2}{M_\pi^2}\right],$$
$$\lambda_0=\frac{M_\pi^2}{Q^2}\left[\frac{f_0(Q^2)}{f_0(0)}-1\right],\quad \zeta(0)=\frac{F_-(0)}{F_+(0)}, \tag{2.11}$$
$$f_0(Q^2)=F_+(Q^2)+\frac{Q^2}{M_K^2-M_\pi^2}F_-(Q^2).$$

On the basis of $K^+_{\mu 3}$, $K^0_{\mu 3}$, K^+_{e3}, and K^0_{e3} data, these coefficients were limited[39] by

$$0.018\le\lambda_+\le 0.039;$$
$$-0.010\le\lambda_0\le 0.028,$$
$$-0.39\le\zeta(0)\le -0.03.$$

The theoretical results are summarized in Table I.

Case (3) seems to be comfortable within the experimental limits. The mock masses appear here as some kind of auxiliary parameters, which take into account the Goldstone-boson nature of the pion.

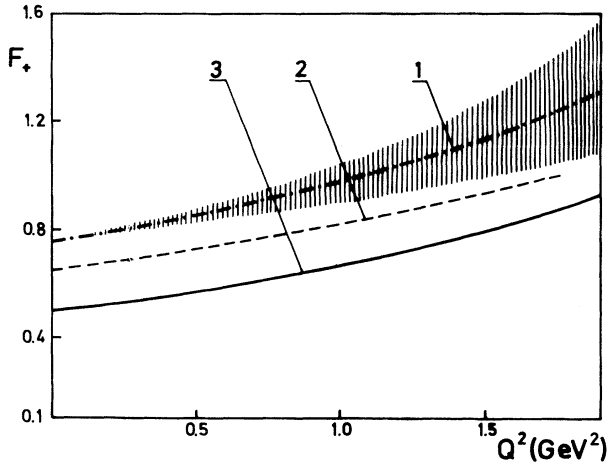

FIG. 5. Form factor $F_+(Q^2)$ for the $D\to K$ transition is compared with the monopole fit from Ref. 41. The shaded region is allowed by monopole formula. Curves are (1) Best fit of Ref. 3; (2) $\tilde{M}_\pi$, $\tilde{M}_K$, $Z=1$; (3) M_π, M_K, $Z=1$.

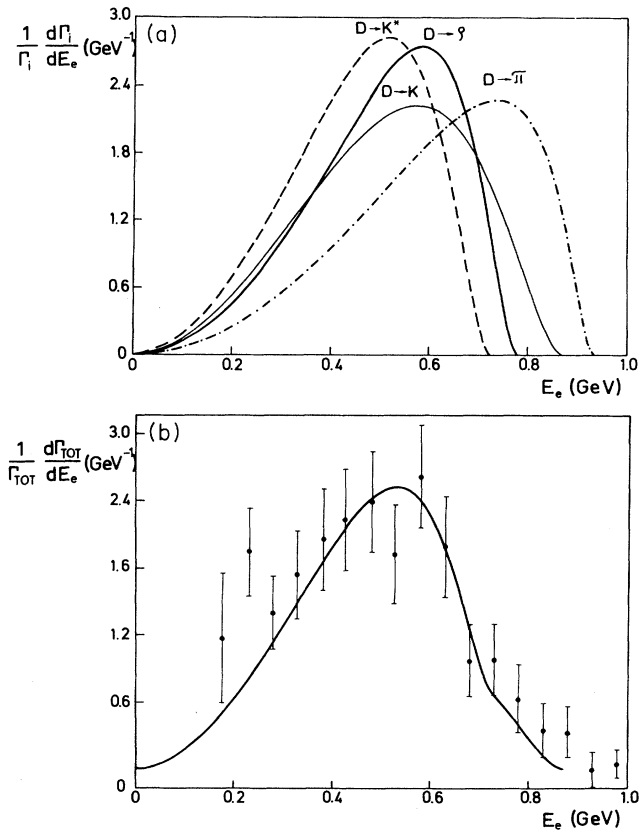

FIG. 6. (a) Shows normalized spectra for semileptonic D decay to K, K^*, π, and ρ mesons. (b) The theoretical spectrum for the D decay to K and K^* mesons is compared with DELCO data (Ref. 45).

TABLE IV. Form factors for $B \to D(D^*)$ decays.

Model	$Q^2=Q^2_{\max}$ $B \to D$ F_+^{SV}	F_-^{SV}	$B \to D^*$ g^{SV}	f^{SV}	a_+^{SV}	a_-^{SV}
Nonrelativistic[a]	1.137	−0.542	1.118	0.894	−1.118	1.118
Breit frame[b]	1.122	−0.536	0.917	0.704	−0.894	0.907
c.m. frame [b]	1.117	−0.525	0.936	0.704	−0.901	0.919
M's physical $R=5$ GeV^{-1}	1.001	−0.88	1.166	0.878	−1.120	1.146
M's physical $R_D=2.77$ GeV^{-1} $R_{D^*}=4.16$ GeV^{-1} $R_B=2.88$ GeV^{-1}	1.122	−0.536	0.917	0.704	0.892	0.907

[a]From Refs. 20 and 41, compiled by Ref. 30.
[b]Reference 30 uses $R_D=2.77$ GeV^{-1}, $R_{D^*}=4.16$ GeV^{-1}, and $R_B=2.88$ GeV^{-1}.

In all tested cases the overlap factor $Z(Q^2)$, which naturally emerges from our theoretical scheme, improves agreement with experimental data. The $Z=1$ approximation was included in our investigations, because it was found (see Secs. III and IV) that it leads to better agreement with the results obtained in some alternative theoretical models. It also works better for $D \to K(K^*)$ and $B \to D(D^*)$ transitions, as will be discussed below.

III. EXCLUSIVE SEMILEPTONIC D-MESON DECAYS

The semileptonic decay modes $M_1 \to M_2$ (pseudoscalar) and $M_1 \to M_2^*$ (vector are described by the following set of invariant form factors:

$$\langle M_2(p_1)|V^\mu|M_1(p_2)\rangle = F_+(p_1+p_2)^\mu + F_-(p_1-p_2)^\mu , \quad (3.1)$$

and

$$\langle M_2^*(p_1)|(V^\mu + A^\mu)|M_1(p_2)\rangle = g\epsilon^{\mu\nu\rho\sigma}\epsilon_\nu^*(p_1+p_2)_\rho(p_1-p_2)_\sigma + f\epsilon^{*\mu} + a_+(\epsilon^*\cdot p_1)(p_1+p_2)^\mu + a_-(\epsilon^*\cdot p_1)(p_1-p_2)^\mu . \quad (3.2)$$

Here all form factors are functions of the momentum transfer $Q^2=(p_1-p_2)^2$, while $\epsilon^\mu=\epsilon^\mu(p_1)$ is the polarization vector of ρ or K^* vector mesons. Our definitions of form factors are compared with definitions of other authors in the Appendix. In Table II we list values of the form factor F_+ for $Q^2=0$ and for $Q^2_{\max}=(M_1-M_2)^2$. They were calculated with physical meson masses for $Z\neq 1$ and $Z=1$. The overlap factor (2.6) ($Z\neq 1$) influences the form-factor values at all $Q^2<Q^2_{\max}$, especially at $Q^2=0$. Table II also includes a comparison with the results published by Ref. 20. Analogous results for the form factors f, g, and a_+ are shown in Table III.

One can see that two models, which are quite dissimilar, agree well for heavy mesons. Without the overlap correction ($Z=1$), the agreement with Ref. 20 is even better. It seems that the dominant ingredient in both models might be the assumption that mesons can be reasonably described by the Fock states containing valence quarks. In such a theoretical scheme, the spectator quark is spin inert.[24]

The valence quarks which constitute our Fock state should be considered as (constituent) effective quarks, which include in their parameters, to some extent, gluon, and quark-antiquark clouds.[20] A more exact theoretical method would include such contributions as additional Fock states.[16,40]

By studying the exclusive decay mode $D^0 \to K^- e^+ \nu_e$, Ref. 41 has concluded that the form factor F_+ can be ap-

TABLE V. Decay rates $\hat{\Gamma}=\Gamma/|V_{cb}|^2$ ($\times 10^{13}$ s^{-1}).

Model	$B \to D$ $\hat{\Gamma}_L^0$	$\hat{\Gamma}_T^1$	$B \to D^*$ $\hat{\Gamma}_L^1$	$\hat{\Gamma}^1=\Gamma_T^1+\hat{\Gamma}_L^1$	$\hat{\Gamma}_L^1/\hat{\Gamma}_T^1$
Bag (1)[a]	1.12	0.73	0.63	1.36	0.86
Bag (2)[a]	1.22	0.92	1.06	1.92	1.15
Ours[b,c]	1.015	0.828	0.914	1.74	1.103

[a]From Ref. 30.
[b]$R_D=2.77$ GeV^{-1}, $R_D=4.16$ GeV^{-1}, and $R_B=2.88$ GeV^{-1}.
[c]$\hat{\Gamma}_{\text{tot}}=\hat{\Gamma}_L^0+\hat{\Gamma}^1$.

TABLE VI. Decay rates for radii $R=2.5$ and 5 GeV^{-1}, $\Gamma=\Gamma/|V_{ij}|^2$ (10^{13} s^{-1}),[a] and $Z=1$.

	$\hat{\Gamma}^0_L$	$\hat{\Gamma}^1_{T+}$	$\hat{\Gamma}^1_{T-}$	$\hat{\Gamma}^1_T$	$\hat{\Gamma}^1_L$	$\hat{\Gamma}^1$	α
$B\to D$	1.005						
	1.026						
$B\to D^*$		0.277	0.922	1.198	1.347	2.545	1.247
		0.280	0.995	1.275	1.397	2.672	1.191
$B\to\pi$	5.09×10^{-2}						
	6.72×10^{-2}						
$B\to\rho$		8.16×10^{-2}	0.917	0.998	0.880	1.878	0.762
		4.73×10^{-2}	0.900	0.946	0.671	1.617	0.418

[a]Upper number is for $R=2.5$ GeV^{-1}, lower for $R=5$ GeV^{-1}.

proximately fitted by a single pole form

$$F_+(Q^2)=F_+(0)\frac{\kappa^2}{\kappa^2+Q^2}\ ,$$
$$\kappa=(2.1^{+0.4}_{-0.2})\ \text{GeV}\ . \tag{3.3}$$

In combination with the D^0 lifetime measurement,[42] they[41] have obtained

$$\Gamma=(D^0\to K^-e^+\nu_e)$$
$$=(9.1\pm1.1\pm1.4)\times10^{+10}\ \text{s}^{-1}\ . \tag{3.4}$$

Both results represent a severe test of our model. As can be seen in Fig. 5, the theoretical F_+ with mock masses (i.e., $\tilde{M}_D,\tilde{M}_K$) and $Z=1$ can reproduce the monopole fit (3.3) with an accuracy of between 3% and 15%, when compared to the largest κ value ($\kappa=2.5$ GeV). However, with mock masses the form factor cannot be defined in the whole physical Q^2 interval. In all other cases, form factors are always too small. With physical mass and $Z=1$, the F_+ values are off by about 11–50 %.

The calculation of the semileptonic partial rate (see the Appendix) gives a similar picture. One finds, for example,

$$(M_D,M_K,\ Z\neq1),\quad \Gamma=|V_{cs}|^2 2.17\times10^{10}\ \text{s}^{-1}\ , \tag{3.5a}$$

$$(M_D,M_K,\ Z=1),\quad \Gamma=|V_{cs}|^2 6.14\times10^{10}\ \text{s}^{-1}\ . \tag{3.5b}$$

As $V_{cs}\sim1$, the $Z=1$ cases are obviously favored by experiment. From (3.4) and (3.5b), one can deduce

$$1.04\le|V_{cs}|\le1.37\ . \tag{3.6}$$

This is close enough to the model-dependent[16,20,43,44] result $|V_{cs}|\sim1.01$ mentioned in Ref. 41. The lowest value in (3.6) is about 6% larger than a guessed "experimental" value[41] $|V_{cs}|=0.975$.

Further comparison with Ref. 20 and with DELCO data[45] is presented in Figs. 6(a) and 6(b). Our spectra, obtained with physical masses and with $Z=1$, are quite close to those calculated by Ref. 20. The theoretical spectrum for the decay $D\to K,K^*$ agrees with the data[45] about as well as Ref. 20.

One can also calculate the ratio of the decay widths for $M_1\to M_2+$ (leptons) transitions:

$$r=\frac{\Gamma(D\to K^*)}{\Gamma(D\to K)+\Gamma(D\to K^*)}\ . \tag{3.7}$$

Our result

$$r=0.54 \tag{3.8}$$

is in perfect agreement with Ref. 20, where one finds $r=0.53$. It is also compatible with their[20] quoted experimental value $r=0.49\pm0.12$.

IV. EXCLUSIVE SEMILEPTONIC B-MESON DECAYS

The invariant form factors are defined by (3.1). The corresponding theoretical expressions are determined by (2.6) and shown in the Appendix. They are different from most other approaches,[16–29,31] having some similarity with Ref. 30. That paper stands in the same relation to our formalism as their earlier papers.[3,46] The option called the "Breit frame" by Ref. 30 corresponds to our hypersurface (2.7). The "c.m. frame" of Ref. 30 would be obtained in our formalism by using the hypersurface defined by

$$\beta_i\cdot z=0\ ,$$
$$i\sim\text{initial}\ . \tag{4.1}$$

Thus both "frames" of Ref. 30 would emerge from a co-

TABLE VII. Product of form factors for $B\to D^*$ decay, the following quark masses are used: $m_u=m_d=0$, $m_c=1.8$ GeV, and $m_b=5$ GeV.

$f(Q^2_{\max})a_+(Q^2_{\max})$[a]	$f(0)a_+(0)$		Model parameters
	-0.26	$Z\neq1$	
-0.984			M's physical
	-0.60	$Z=1$	
	-0.28	$Z\neq1$	
-1.008			$\tilde{M}$'s mock
	-0.55	$Z=1$	

[a] Isgur's (Ref. 16) form factors are used because they correspond to the Altomari-Wolfenstein (Ref. 22) form factors: See Table X.

TABLE VIII. Decay rates for radius $R=5$ GeV, $Z=1$, and $Z\neq 1$ (upper number is for $Z=1$, lower for $Z\neq 1$); $\hat{\Gamma}=\Gamma/|V_{ij}|^2$ (10^{13} s^{-1}) for B decays, (10^{11} s^{-1}) for D decays.

	$\hat{\Gamma}^0_L$	$\hat{\Gamma}^1_{T^+}$	$\hat{\Gamma}^1_{T^-}$	$\hat{\Gamma}^1_T$	$\hat{\Gamma}^1_L$	$\hat{\Gamma}^1$	α
$B\to D$	1.026						
	0.523						
$B\to D^*$		0.280	0.995	1.275	1.397	2.672	1.191
		0.205	0.675	0.880	0.851	1.731	0.935
$B\to\pi$	0.0672						
	0.0012						
$B\to\rho$		0.047	0.899	0.946	0.671	1.617	0.418
		0.023	0.253	0.275	0.150	0.425	0.087
$D\to K$	0.614						
	0.217						
$D\to K^*$		0.086	0.252	0.339	0.384	0.722	1.264
		0.071	0.199	0.270	0.283	0.553	1.091
$D\to\pi$	0.153						
	0.010						
$D\to\rho$		0.082	0.322	0.404	0.431	0.836	1.133
		0.063	0.230	0.293	0.281	0.575	0.919

variant theory, but each corresponds to a different dynamical assumption. The hypersurface (2.7), for example, is compatible with the CVC constraint, while the hypersurface (4.1) is not. In Ref. 30 form factors were calculated at $Q^2=Q^2_{\max}$ and then inserted into a vector-meson-dominance-inspired monopole formula. A further comparison is given in Table IV, which is an enlarged version of Table II in Ref. 30. Our form factors were correlated with Lie-Svendsen[30] form factors using Table X from the Appendix.

The numbers in Table IV illustrate the influence of MB model parameters. The row labeled "Breit frame" was calculated in a model[30] which is almost identical with ours. However, with different MB model parameters, our results (labeled "M's physical") agree much better with the first row of Table IV. The same agreement with Refs. 20 and 41 has already been demonstrated in Fig. 5 and 6. Using the same parameters as Ref. 30, we have obtained the results identical with the Breit frame row in Table IV. All values in Table IV were obtained with the $Z=1$ approximation.

However, equal form factors at $Q^2=Q^2_{\max}$ do not lead to equal predictions for decay rates. In one case[30] a pole form was assumed for the Q^2 dependence of the form factors. In our case this dependence was directly calculated from our model, with the $Z=1$ approximation. Respective results are compared in Table V. For $B\to D^*$ transitions, BBM-based values fall between bags 1 and 2 values of Ref. 30, being roughly about 28% or 10% smaller or larger, respectively. This is of the same order of magnitude as the differences caused by variations of model parameters. The decay rates for $B\to D$ transitions show similar disagreements. The theoretical results in Table V are about $\frac{1}{2}$ of the spectator-model prediction for the total decay rate:

$$\hat{\Gamma}_{\rm tot}=\Gamma_{\rm tot}/|V_{cb}|^2=5.6\times 10^{13}\ {\rm s}^{-1}\ . \tag{4.2}$$

Our estimate for $|V_{cb}|$, based on the results from Table V and on the measured lifetime,[47] is close to their[30] value:

$$\begin{aligned} &|V_{cb}|=0.058,\ \text{ours}\ (Z=1)\ , \\ &|V_{cb}|=0.05,\ \ \text{Ref. 30}\ . \end{aligned} \tag{4.3}$$

The mixing angle value is influenced not only by the bag radius, but by the overlap factor also. For $R_B=R_D=R_{D^*}=5$ GeV^{-1}, we have found

$$0.053\leq|V_{cb}|\leq 0.068\ . \tag{4.4}$$

The first value was obtained using $Z=1$, while the second value followed when $Z(Q^2)\neq 1$ was entered.

The parameter α, which appears in the angular distribution (4.10), discussed below, is quite insensitive to R values. One obtains

$$\begin{aligned} &\alpha=1.206\ (R\text{'s from Ref. 30; see Table IV})\ , \\ &\alpha=1.247\ (\text{all } R\text{'s}=2.5\ \text{GeV}^{-1})\ , \\ &\alpha=1.191\ (\text{all } R\text{'s}=5\ \text{GeV}^{-1})\ . \end{aligned} \tag{4.5}$$

Our ratio $\hat{\Gamma}^1_L/\hat{\Gamma}^1_T$ in Table V is in reasonable agreement with the ARGUS Collaboration measurement[48]

$$\hat{\Gamma}^1_L/\hat{\Gamma}^1_T=0.85\pm 0.45\ . \tag{4.6}$$

The choice of meson radii is more important for light mesons than for more massive mesons. In Table VI one can see that a drastic change of the universal meson radius from $R=5$ to 2.5 GeV^{-1} can change the $B\to\rho$ decay rates by factor $1.7(\Gamma_{T^+})$. However, $B\to D(D^*)$ decay rates change by less than 10%. Such a parameter dependence serves as a very good indicator for the theoretical accuracy of the model-based predictions. When only massive $B(B^*)$ and $D(D^*)$ mesons are involved, it could be about 2–10 %.

Reference 23 has emphasized the importance of Lorentz covariance. They have found

$$f(Q^2_{\max})a_+(Q^2_{\max})=-1\ . \tag{4.7a}$$

Ours results are quite close to that value, as shown in Table VII. One inevitably obtains $fa_+<0$, which might be at variance with the preliminary experimental results.[23] The absolute magnitude of the product fa_+ depends on the momentum transfer Q^2, which is easily calculated in our model. The results for $Q^2=0$ are also displayed in Table VII. An entirely different approach[18] based on QCD sum rules found

$$f(0)a_+(0)=-0.4\ . \tag{4.7b}$$

This seems to be in reasonable agreement with Table VII, which is quite encouraging. The value (4.7b), which was obtained by using quite different theoretical methods,[18] falls between our $Z=1$ and $Z\neq 1$ values.

It is interesting that most other[18,24] results also fall between our cases $Z=1$ and $Z\neq 1$, as one can see from the following. It could be that higher Fock states, containing $q\bar{q}$ pairs and gluons, for example, would conspire against the effect of the $Z\neq 1$ correction factor. On the other hand, $Z\neq 1$ is definitively needed to explain the measured Q^2 dependence of proton and pion electromagnetic form factors (Sec. II).

Our predictions for semileptonic decay rates are shown in Table VIII for both $Z=1$ and $Z\neq 1$, using physical (M) meson masses. (Table VIII contains both D- and B-meson decay rates.) The theoretical expressions for $d^2\Gamma/dQ^2dE_e$ can be found in the Appendix, where we also compare physical and mock-meson masses showing that they differ only by a little for massive mesons.

In Fig. 7 one can see theoretical spectra $(1/\Gamma)(d\Gamma/dE_e)$ for B-meson decays, which show remarkable similarity with Ref. 20.

Our values for the semileptonic decay rates are compared with the data of Ref. 24 and with some earlier calculations in Table IX.

The poorest agreement is with the nonrelativistic calculations. There is good agreement with Ref. 24. Their values always fall between our $Z=1$ and $Z\neq 1$ results. In all models the ratio

$$r=\frac{\Gamma(B\to D^*)}{\Gamma(B\to D^*)+\Gamma(B\to D)} \tag{4.8}$$

is compatible with the experimental value[49]

$$r=0.85\pm 0.32\ . \tag{4.9}$$

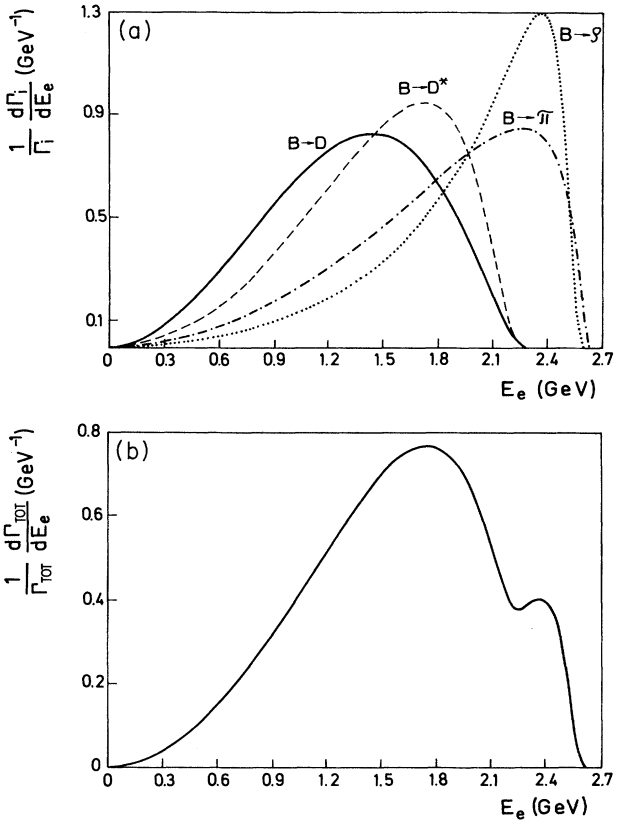

FIG. 7. (a) Shows normalized spectra for semileptonic B decays to D, D^*, π, and ρ mesons. (b) Shows theoretical spectrum for the B decay into D, D^*, π, and ρ channels.

TABLE IX. Semileptonic decay rates for $B\to D,D^*$, $\hat{\Gamma}=\Gamma/|V_{bc}|^2$ (10^{12} s^{-1}).

	$\hat{\Gamma}^1_{T^-}$	$\hat{\Gamma}^1_{T^+}$	$\hat{\Gamma}^1_L$	$\hat{\Gamma}^0_L$	$\hat{\Gamma}^1_{T+L}$	$\hat{\Gamma}^{0+1}_{T+L}$	$\frac{\Gamma_{D^*}}{\Gamma_D}$	r	α
FQD[a]	10.0	2.4	24.8		37.1				
Mode	$B\to D^*$	$B\to D^*$	$B\to D^*$	$B\to D$	$B\to D^*$	$B\to D+D^*$			$B\to D^*$
GIW[b]	11.6	3.0	35.0	14.3	49.6	63.9	3.5	0.78	3.83
PS[c]	8.2	8.2	52.4	7.2	68.8	76.0	9.6	0.91	5.83
KS[d]	9.8	2.9	13.1	8.3	25.8	34.1	3.1	0.76	1.06
$M,Z=1$	9.95	2.80	13.97	10.26	26.68	36.95	2.60	0.722	1.191
$M,Z\neq 1$	6.75	2.05	8.51	5.23	17.31	22.54	3.31	0.768	0.935

[a]FQD means free-quark decay $b\to c+e^-+\bar{\nu}_e$.
[b]References 16, 50, and 51.
[c]Reference 21.
[d]Reference 24.

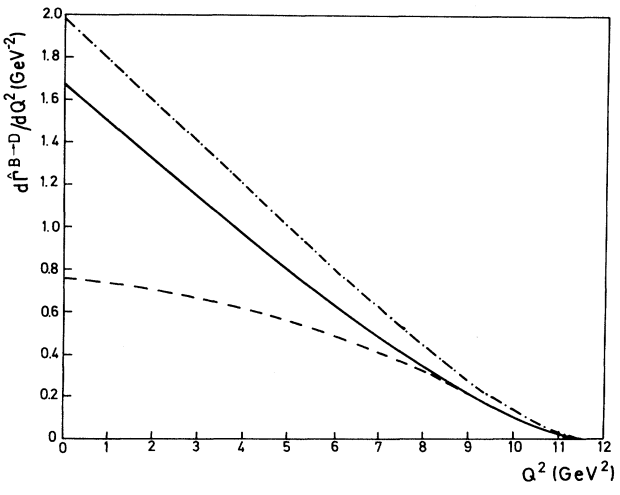

FIG. 8. Differential Q^2 distribution of semileptonic $B\to D$ decay. Solid curve is the one given by Ref. 24. The dot-dashed curve corresponds to $Z=1$. The dashed curve was calculated with $Z(Q^2)\neq 1$. Here $\hat{\Gamma}=\Gamma/(|V_{bc}|^2\times 10^{12}\ s^{-1})$.

In Figs. 8 and 9 our differential Q^2 distributions $d\Gamma/dQ^2$ of semileptonic B-meson decays are compared with the corresponding curves of Ref. 24. For the $Z=1$ case the disagreement is always less than 20%.

In general, our model agrees better with Ref. 24 than with some other approaches. $d\Gamma/dQ^2$ values of Ref. 24, for example, are 4 or 2.7 times smaller than the value given in Refs. 16, 21, 50, and 51.

It is also very useful to study the angular distribution

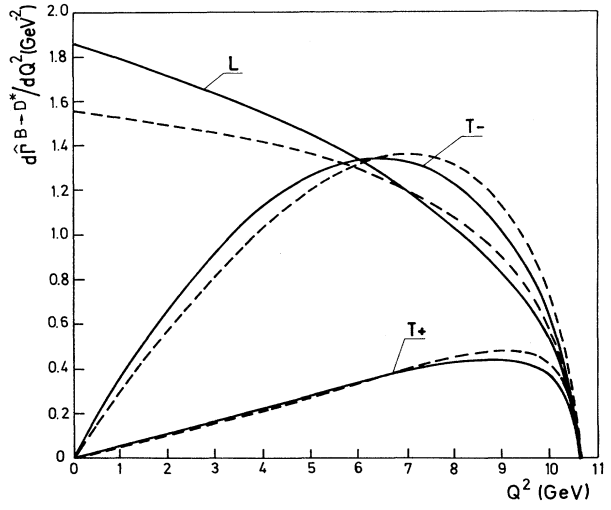

FIG. 9. Differential Q^2 distributions of semileptonic $B\to D^*$ decay for transverse ($T_\pm$) and longitudinal (L) contributions. The solid line is our ($Z=1$) calculation. The dashed line is from Ref. 24. $\hat{\Gamma}$ is as in Fig. 8.

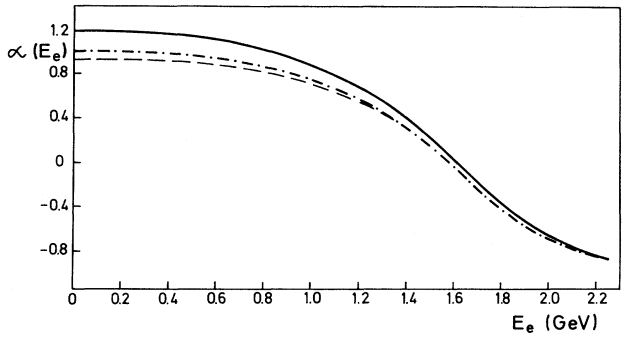

FIG. 10. Values of asymmetry parameter α [Eq. (4.10)] are plotted as a function of the lowest measured lepton energy (momentum) E_e. Solid curve is our values for $Z=1$ and the dashed curve for $Z(Q^2)\neq 1$. The dot-dashed curve is from Ref. 24.

of the strong decay $D^*\to D\pi$, which appears in the sequence

$$\bar{B}_0\to D^{*+}+l^-+\bar{\nu}$$
$$\quad\ \ \hookrightarrow D^0\pi^+ .$$

Reference 24 gives the angular distribution[52]

$$W(\cos\theta)=(1+\alpha\cos^2\theta)\frac{3}{6+2\alpha} . \tag{4.10}$$

Here θ is the polar angle of the D (or π) meson in the D^* rest frame with respect to the D^* direction in the laboratory frame. The theoretical expression for the coefficient α is given in the Appendix.

In Fig. 10 the value of the coefficient α is shown as a function of the lowest measured[52] lepton energy (momentum) E_e. Our results are in remarkably good agreement with the curve obtained by using the model of Ref. 24. Their curve lies between our two cases $Z=1$ and $Z\neq 1$. For $E_e=1.4$ GeV, one has

$$\begin{aligned}&\alpha\ (Z=1)=0.40 ,\\ &\alpha\ (Z\neq 1)=0.31 ,\\ &\alpha\ (\text{Ref. 24})=0.32 ,\\ &\alpha\ (\text{Ref 16})=0.28 .\end{aligned} \tag{4.11}$$

Any of those numbers can be compatible with the measured value[52]

$$\alpha=0.65\pm 0.66\pm 0.25 . \tag{4.12}$$

V. CONCLUSION

A simple quark model, namely, the MIT bag model, was made relativistic in the simplest possible way, which still ensures full Lorentz covariance. In the static limit ($\mathbf{P}=0$), our model goes into the MIT bag model and thus retains all bag model parameters. These parameters, together with a hyperplane selection, completely specify the model.

TABLE X. Form factors.

This work	Reference 24	16	20	30
$F_+\delta^*$	F_+^V	f_+	h_1	f_+
$f\delta$	F_i^A	f	$h_{A1}M_S$[a]	fM_S
$2a_+\delta$	F_2^A	$2a_+$	$-2h_A2M_S^{-1}$	$2a_+M_S^{-1}$
$-2g\delta$	F^V	$-2g$	$-2h_VM_S^{-1}$	$-2gM_S^{-1}$

[a]$\delta=(4M_iM_f)^{1/2}$, $M_S=M_i+M_f$.

TABLE XI. Meson masses.

Meson	Mass (GeV) Physical	Mock
π	0.135	0.817
ρ	0.770	0.817
K	0.494	0.979
K^*	0.892	0.979
D	1.87	2.305
D^*	2.01	2.305
B	5.27	5.45
Proton	0.938	1.223

A similar procedure could work for any model based on a central confining potential, which must depend on $z_\mu^\perp(P)$. The often used potential $V(r)=(1+\gamma^0)f(r)$, for example, is, from our point of view, the rest-frame form of the potential

$$V(z^\perp(P))=(1+\gamma\cdot L)f(z^\perp(P)) .$$

It is quite surprising that such a simplified picture of the quark dynamics, with hadron states containing valence quarks only, can approximate proton form factors up to $Q^2=1.40$ GeV. The model is less successful with pions where the valence-quark approximation is a poor one.

An interesting feature of our model is the appearance of the overlap factor Z (2.6), which is essential in the calculation of proton form factors. Heavy D- and B-meson decays seem to be better described without this factor, i.e., with $Z=1$. This approximation was also used by Ref. 30. As this procedure is not consistent with the construction of the model, it has to be considered as an additional *ad hoc* adjustment, akin to the auxiliary fitting parameters used in some models.[16,20,21]

Formally speaking, our model can calculate form factors up to any Q^2. However, above certain Q^2 the simple physical assumptions, used in the building of the model, are no longer adequate and the agreement with empirical data worsens.

The model predictions agree reasonably well with other approaches,[16,18–31] although some of them are based on entirely different theoretical schemes.

An important bag model parameter is the bag radius R, which differs from hadron to hadron, so that form factors could depend strongly on its precise value. However, numerical checks show (see Tables V and VI) that BBM results are quite stable against the changes of radii. By going from $R=5$ GeV for both B and D (D^*) mesons to $R=2.88$ GeV for the D (D^*) meson, theoretical widths change for about 3%. However, when the process involves a lighter meson, π or ρ, results can change, in some cases, by a factor of 2.

Nevertheless, it seems that, aside from the puzzling $Z=1$ adjustment, the BBM need not rely on the fine-tuning of its parameters. All of them can be fixed by the data (masses, etc.) usually described in the standard MIT bag model. With such parameters the BBM provides a simple approximate description of the hadron form factor at lower Q^2 values.

APPENDIX

The full expressions for meson form factors in the Breit frame are

$$F_+=F_{\rm fl}Z\frac{1}{4M_iM_fuu^0}\left[\frac{u}{u^0}(M_S)I_{\gamma^0}+(M_D)I_{\gamma,1}\right] , \tag{A1}$$

$$F_-=F_+(M_S\leftrightarrow -M_D) , \tag{A2}$$

$$f=F_{\rm fl}Z\frac{1}{u^0}I_{\gamma\gamma_5,1} , \tag{A3}$$

$$a_+=F_{\rm fl}Z\frac{1}{8M_i^2M_fu^{02}u}\left[(M_S)\left[\frac{1}{u^0}I_{\gamma^0\gamma_5}-\frac{u}{u^0}I_{\gamma\gamma_5,1}\right]+(M_D)\left[\frac{1}{u}I_{\gamma\gamma_5,2}-\frac{u^0-1}{u}I_{\gamma\gamma_5,1}\right]\right] , \tag{A4}$$

$$a_-=a_+(M_S\leftrightarrow -M_D) , \tag{A5}$$

$$g=F_{\rm fl}Z\frac{1}{4M_iM_fu^{02}u}I_{\gamma,2} . \tag{A6}$$

Here Z are overlap factors given by (2.6), M_i,M_f are meson masses, $u^0=E_f/M_f$ and $u=|\mathbf{P}_f/M_f|$ correspond to the four-velocity, $u_f^\mu=p_f^\mu/M_f$, $M_S=M_i+M_f$, and $M_D=M_i-M_f$.

The integrals over radial quark wave functions are

$$
\begin{aligned}
I_{\gamma^0} &= \int dl \cos[\arg(I)][U_f(r)U_i(r)+V_f(r)V_i(r)] ,\\
I_{\gamma,1} &= I_{\gamma^0\gamma_5} = \int dl \sin[\arg(I)][U_f(r)U_i(r)-V_f(r)V_i(r)]\cos\theta ,\\
I_{\gamma,2} &= \int dl \{\cos[\arg(I)][U_f(r)U_i(r)-\cos^2\theta V_f(r)V_i(r)]u_1\\
&\quad -\sin[\arg(I)][U_f(r)U_i(r)+V_f(r)V_i(r)]u_1^0\cos\theta\} ,\\
I_{\gamma\gamma_5,1} &= I_{\gamma,2}(u_1^0 \leftrightarrow u_1) ,\\
I_{\gamma\gamma_5,2} &= \int dl \{\cos[\arg(I)][U_f(r)U_i(r)(1-u_1^0)+V_f(r)V_i(r)][(2\cos^2\theta-1)+u_1^0\cos^2\theta]\\
&\quad +\sin[\arg(I)][U_f(r)U_i(r)+V_f(r)V_i(r)]u_1\cos\theta\} .
\end{aligned}
\tag{A7}
$$

The radial quark wave functions are defined by (3.5), where χ is a Pauli spinor.

The connection between our form factors and some other formalisms are shown in Table X.

In Table XI we list physical and mock-meson masses. The mock masses were calculated with quark energies, which (bag radius $R=5$ GeV^{-1}) are (in GeV) $\epsilon_{u,d}=0.4086$, $\epsilon_s=0.5705$, $\epsilon_c=1.896$, and $\epsilon_b=5.038$. The quark masses were $m_{u,d}=0$, $m_s=0.279$, $m_c=1.8$, and $m_b=5$.

The double differential decay distribution[24] for $M_i \to M_f$ or M_f^* is given by

$$
\begin{aligned}
\frac{d\Gamma[M_i \to M_f(M_f^*)]}{dQ^2 dE_e} &= \frac{G^2}{(2\pi)^3}\frac{1}{16}\frac{Q^2}{M_i^2}[(1-\cos\tilde\theta)^2|H_-|^2+(1+\cos\tilde\theta)^2|H_+|^2+2(1-\cos^2\tilde\theta)|H_0|^2]\\
&= \frac{d\Gamma_{T^-}}{dQ^2 dE_e}+\frac{d\Gamma_{T^+}}{dQ^2 dE_e}+\frac{d\Gamma_L}{dQ^2 dE_e} .
\end{aligned}
\tag{A8}
$$

Here $\tilde\theta$ is the polar angle between the M_f (M_f^*) and the lepton l^- in the ($l^-\bar\nu_l$) center-of-mass (c.m.) system where

$$2M_i p\cos\tilde\theta = M_i^2 - M_f^2 + Q^2 - 4M_i E_e ,$$

and p is c.m. momentum of the final-state meson.

The factors H in (A8) are given by

$$
\begin{aligned}
H_0^M &= \frac{p}{(Q^2)^{1/2}} 2M_i \delta F_+ ,\\
H_\pm^{M^*} &= \delta f \mp m_i p R\, 2\delta g ,\\
H_0^{M^*} &= \frac{1}{2M_f (Q^2)^{1/2}}[(M_i^2 - M_f^2 - Q^2)\delta f + 2M_i^2 p^2 2\delta a_+] ,\\
\delta &= (4M_i M_f)^{1/2} .
\end{aligned}
\tag{A9}
$$

The superscript labels the decay into a pseudoscalar (M) or a vector (M^*) meson.

[1] T. Biswas and F. Rohrlich, Nuovo Cimento A **88**, 57 (1985).
[2] V. Dananić, D. Tadić, and M. Rogina, Phys. Rev. D **35**, 1698 (1987).
[3] A. Ilakovac and D. Tadić, Z. Phys. C **44**, 119 (1989).
[4] A. Ilakovac, Fizika **20**, 261 (1988).
[5] M. V. Barnhill III, Phys. Rev. D **20**, 729 (1979).
[6] I. Picek and D. Tadić, Phys. Rev. D **27**, 665 (1983).
[7] W.-Y. P. Hwang, Z. Phys. C **16**, 327 (1983).
[8] M. Betz and R. Goldflam, Phys. Rev. D **28**, 2848 (1983).
[9] P. A. M. Guichon, Phys. Lett. **29B**, 108 (1983).
[10] Ch. Hajduk and B. Schwesinger, Nucl. Phys. **A423**, 419 (1984).
[11] X. M. Wang and P. Ch. Yin, Phys. Lett. **140B**, 249 (1984).
[12] X. M. Wang, Phys. Lett. **140B**, 413 (1984).
[13] A. O. Gattone and W. Y. P. Hwang, Phys. Rev. D **31**, 2874 (1985); Indiana University report (unpublished).
[14] A. L. Licht and A. Pagnamenta, Phys. Rev. D **2**, 1150 (1970).
[15] N. Isgur and C. H. Llewellyn Smith, Nucl. Phys. **B317**, 526 (1989).
[16] N. Isgur, D. Scora, B. Grinstein, and M. B. Wise, Phys. Rev. D **39**, 799 (1989).
[17] B. I. Ioffe and A. V. Smilga, Phys. Lett. **114B**, 353 (1982); Nucl. Phys. **B216**, 373 (1983); V. A. Nestorenko and A. V. Radushkin, Phys. Lett. **115B**, 410 (1982); Pis'ma Zh. Eksp. Teor. Fiz. **35**, 395 (1982) [JETP Lett. **35**, 488 (1982)]; Phys. Lett. **128B**, 439 (1983); Yad. Fiz. **39**, 1287 (1984) [Sov. J. Nucl. Phys. **39**, 811 (1984)]; A. V. Radushkin, Acta Phys. Pol. B **15**, 403 (1984).
[18] A. A. Ovchinikov and V. A. Slobodenyuk, Yad. Fiz. **50**, 1433 (1989) [Sov. J. Nucl. Phys. **50**, 891 (1989)].
[19] H. Leutwyler and M. Roos, Z. Phys. C **25**, 91 (1984).
[20] M. Wirbel, B. Stech, and M. Bauer, Z. Phys. C **29**, 637 (1985).
[21] F. Schöberl and H. Pietschmann, Europhys. Lett. **2**, 583

(1986).
[22]T. Altomari and L. Wolfenstein, Phys. Rev. Lett. **58**, 1583 (1987); Phys. Rev. D **37**, 681 (1988).
[23]E. Golowich, F. Iddir, A. Le Yaouanc, L. Oliver, O. Pène, and J. C. Raynal, Phys. Lett. B **213**, 521 (1988).
[24]J. G. Körner and G. A. Schuler, Z. Phys. C **38**, 511 (1988); Phys. Lett. B **232**, 306 (1989); Z. Phys. C **46**, 93 (1990).
[25]C. A. Dominguez and N. Paver, Z. Phys. C **41**, 217 (1988).
[26]P. Heiliger and I. M. Sehgal, Phys. Lett. B **229**, 409 (1989).
[27]F. J. Gilman and R. L. Singleton, Jr., Phys. Rev. D **41**, 142 (1990).
[28]N. Isgur and M. B. Wise, Phys. Rev. D **41**, 151 (1990).
[29]V. Barger, C. S. Kim, and R. J. N. Phillips, Phys. Lett. B **235**, 187 (1990).
[30]Ø. Lie-Svendsen, Z. Phys. C **45**, 521 (1990).
[31]K. Hagiwara, A. D. Martin, and M. F. Wade, Z. Phys. C **46**, 299 (1990).
[32]A. A. Logunov and A. N. Tavkhelidze, Nuovo Cimento **29**, 380 (1963); A. A. Logunov, A. N. Tavkhelidze, I. T. Todorov, and O. A. Khrustalev, *ibid.* **29**, 134 (1963); R. Blankenbecker and R. Sugar, Phys. Rev. **142**, 1051 (1965); C. Itzykson, V. G. Kadishevsky, and I. T. Todorov, Phys. Rev. D **1**, 2823 (1971).
[33]A. Chodos *et al.*, Phys. Rev. D **9**, 3471 (1974); T. De Grand *et al.*, *ibid.* **12**, 2060 (1975).
[34]H. W. Crater and P. Van Alstine, Ann. Phys. (N.Y.) **148**, 57 (1983); Phys. Rev. D **30**, 2585 (1984), and references therein.
[35]O. Dumbrajs *et al.*, Nucl. Phys. **B216**, 277 (1983); P. N. Kirk *et al.*, Phys. Rev. D **8**, 63 (1973); G. Höhler *et al.*, Nucl. Phys. **B114**, 505 (1076).
[36]M. V. Barhhill, Phys. Rev. D **20**, 723 (1979).
[37]C. J. Bebek *et al.*, Phys. Rev. D **17**, 1693 (1978).
[38]S. R. Amendolia *et al.*, Nucl. Phys. **B277**, 168 (1986).
[39]E. D. Commins and P. H. Bucksbaum, *Weak Interactions of Leptons and Quarks* (Cambridge University Press, Cambridge, England, 1983).
[40]L. C. L. Hollenberg and B. H. J. McKeller, Austr. J. Phys. **42**, 11 (1989); Int. J. Mod. Phys. A **4**, 1949 (1989); Phys. Rev. D **40**, 145 (1989); J. Phys. G **16**, 31 (1990).
[41]J. C. Anjos *et al.*, Phys. Rev. Lett. **62**, 1587 (1989).
[42]J. R. Raab, Phys. Rev. D **37**, 2391 (1988); Ph. D. thesis, University of California, Santa Barbara, Report No. UCSB-HEP-87-8, 1987.
[43]T. M. Aliev, V. L. Eletskii, and Ya. I. Kogan, Yad. Fiz. **40**, 823 (1984) [Sov. J. Nucl. Phys. **40**, 527 (1984)].
[44]C. A. Dominguez and N. Paver, Phys. Lett. B **197**, 423 (1987).
[45]W. Bacino *et al.*, Phys. Rev. Lett. **43**, 1073 (1979).
[46]Ø. Lie-Svendsen and H. Høgaasen, Z. Phys. C **35**, 239 (1987).
[47]Particle Data Group, G. P. Yost *et al.*, Phys. Lett. B **204**, 1 (1988).
[48]H. Albrecht *et al.*, Phys. Lett. B **219**, 121 (1987).
[49]A. Chen *et al.*, Phys. Rev. Lett. **52**, 1084 (1984); E. H. Thorndike, in *Proceedings of the 1985 International Symposium on Lepton and Photon Interactions at High Energies,* Kyoto, Japan, 1985, edited by M. Konuma and K. Takahashi (RIFP, Kyoto University, Kyoto, 1986).
[50]B. Grinstein, M. B. Wise, and N. Isgur, Phys. Rev. Lett. **56**, 298 (1986).
[51]Data in Table V were compiled in Ref. 14.
[52]D. Bortoletto *et al.*, Phys. Rev. Lett. **63**, 1667 (1989).